# FRACTOGRAPHIC ASPECTS OF FATIGUE CRACK GROWTH IN POROUS SINTERED STEELS

B. Karlsson*, J. Wasén* and I. Bertilsson**

The fracture behaviour during fatigue crack propagation in porous sintered steels has been studied. PM-steels produced by atomization techniques with analysis 0.5% Mo, 1.75% Ni and 0.5% C with pore fractions 0.16 and 0.10 were employed in the experiments. Quantitative fractography applied on fracture profiles revealed that the pores constitute the "continuous" phase in the fatigue fracture surface. The cracks propagate in the main between the nearest neighbouring pores in the macroscopic forward direction, synonymous with a wide distribution of crack tip directions. The main crack is surrounded by a zone of microcracks, resulting in unloading of the main crack tip.

## INTRODUCTION

The mechanical properties of sintered steels are highly dependent on the porosity of the material (Karlsson and Bertilsson (1); Exner and Pohl (2); Nakamura and Tsuya (3); Crane and Farrow (4)). The influence of the pore structure on the fatigue crack growth properties has been studied to a rather limited extent (Bertilsson and Karlsson (5); Douib et al. (6); Bertilsson and Karlsson (7)), but the following general observations have been made. An increase of the pore content (i.e. a reduction in the density of the steel) leads to a higher crack propagation rate, da/dN, at a given stress intensity amplitude, $\Delta K$, (5,7) and a decreased fatigue crack growth threshold, $\Delta K_{th}$, (5). The crack closure level, $K_{cl}$, exhibits a high sensitivity to the maximum applied stress intensity, $K_{max}$, during the load cycle (5).

The aim of this paper is to give a qualitative explanation of these facts based on fractographic observations and quantitative fractographic measurements.

* Department of Engineering Metals, Chalmers University of Technology, S-412 96 Göteborg, Sweden
** Materials Technology, Volvo Flygmotor AB, S-461 81 Trollhättan, Sweden

## MATERIALS AND EXPERIMENTAL TECHNIQUES

The ferrous powder used for the production of the materials in the present investigation has the chemical composition 0.5% Mo and 1.75% Ni with balance of Fe. The powder was water atomized from a prealloyed melt, resulting in a homogeneous distribution of the alloying elements. Graphite corresponding to a final carbon content in the material of 0.5% and 0.8% zinc-stearate as lubricant were mixed into the powder before pressing. Two densities, 6600 and 7100 kg/m$^3$ (pore fraction 0.16 and 0.10 respectively), were produced by single pressing. Sintering was performed in a belt furnace at 1120°C for 30 min with endogas as a protective atmosphere. The cooling rate from the sintering temperature was about 1°C/s. The specimens were tested in the as-sintered condition.

The microstructure of the material consists essentially of coarse pearlite with a rather irregular cementite morphology, although minor regions appear with lamellae-shaped cementite. The microhardness (20 g load) of the divorced pearlite is about 270 HV.

The fatigue crack growth tests were performed in tension mode under constant load amplitude with R=0.05. The nominal cross section of the employed SEN specimens was 15x5 mm$^2$ with the fatigue crack propagating in the wide direction. Further experimental details and results have been reported before (7).

In order to study the influence of the porosity on the fatigue crack path, quantitative fractographic analysis was made on the two steels. The fractographic measurements were performed by the aid of profile analysis, i.e. analysis of a fracture line created by a vertical section through the fracture surface along the direction of the propagating crack (Karlsson and Wasén (8)). The parameters used to describe the fracture path are the length distribution of approximating chords between neighbouring pores along the fracture line (Fig. 1a) and the distribution of angles of these chords as related to the macroscopic crack direction (Fig. 1a). The number of chords recorded in the measurements was typically 300 in each case.

## RESULTS AND DISCUSSION

In order to determine the influence of the pores on the local cracking events at the crack tip the measured length distribution of approximating chords, connecting consecutive pores, along the fracture path can be compared to the two extreme cases of crack path geometry corresponding to no or "total" pore control. If the size distribution of these line elements between pores along the fracture line is equal to the size distribution of linear inter-distances between pores in a random direction there is no influence of the pores on the crack path. However, if the chord distribution equals the size distribution of straight line elements connecting the nearest pores in an angular sector embracing ±90° from the macroscopic crack growth direction (cf. Fig. 1b), there is an indication of more or less total local pore control of the fracture.

Measurements along random lines indicated that the intercept lengths between pores approximately follow logarithmic normal distributions for the two materials with mean

values, l', and standard deviations, $\sigma$', according to Table 1. The identical powders used in the two materials together with the experimentally found similarity in the number of pores per unit volume indicate smaller pores in the denser material. These facts explain the difference in the l'- and $\sigma$'-values, respectively, found for the two materials being due to the smaller hitting probability of pores with decreasing size.

The distribution of angles for chords connecting nearest neighbouring pores lying in the forward half plane (angles referred to the macroscopic crack direction, Fig. 1b) turned out to be broad but not uniform. (A uniform angle distribution would correspond to a standard deviation of about 52° (8)). This non-uniformity of the distribution is due to the correlation between the pores created during the powder packing; cf. the pore distribution in Fig. 2b. The standard deviation of this angle distribution, $\theta$", is virtually independent of the volume fraction of pores (Table 1). The length distribution of these chords connecting the nearest neighbouring pores in the defined macroscopic "forward" direction $\pm 90°$ is logarithmic normal distributed with mean value l" and standard deviation $\sigma$" (Fig. 1b, Table 1). The mean value l" shows a porosity dependence in the same manner as the mean intercept length l' between pores in a random direction (Table 1).

TABLE 1 - Geometrical data.

| Parameter | Pore fraction 0.16 | Pore fraction 0.10 | Remarks |
|---|---|---|---|
| l' ($\mu$m) | 50.3 | 70.0 | Pores along random lines |
| $\sigma$' ($\mu$m) | 44.8 | 58.6 | |
| l" ($\mu$m) | 11.0 | 14.2 | Neighbouring pores along the macroscopic crack growth direction $\pm 90°$ |
| $\sigma$" ($\mu$m) | 7.9 | 10.2 | |
| $\theta$" (deg) | 42 | 45 | |
| l ($\mu$m) | 9.4 | 15.8 | Pores along the fracture line |
| $\sigma$ ($\mu$m) | 7.7 | 11.4 | |
| $\theta$ (deg) | 47 | 47 | |

The angle distribution of the approximation chords between consecutive pores *along the fracture path* (Fig. 1a) and the macroscopic main fracture plane is unaffected by the density and its standard deviation $\theta$ is similar to $\theta$" (Table 1). In comparison, corresponding angle deviations of approximating chords along fracture profiles in fully dense ferritic steels (Karlsson and Wasén (9)) are much smaller, $\theta$ being typically 35 degrees.

The mean interdistance between consecutive pores along the fracture path is logarithmic normal distributed with mean value l and standard deviation $\sigma$ (Table 1). The mean value of the distribution increases with decreasing porosity (Table 1). When comparing l with l' (corresponding to the mean interdistance along a random line) it is obvious that l in both cases is approximately five times smaller than l'. This observation excludes the possibility

that the fracture is unaffected by the pore structure. A comparison between l and l" (corresponding to mean nearest neighbour distances between pores in a "forward" direction), on the other hand, shows that they are approximately equal indicating a very strong pore control of the fracture.

No significant dependence on the maximum applied stress intensity was found for the distributions of chord angles, $f(\theta)$, or interdistances between consecutive pores, g(l), along the fracture profile.

The crack propagation behaviour in porous sintered steels is different from fully dense steels in the sense that the crack is non-continuous in sintered steels (Fig. 2a). If a fracture surface is studied, it is seen that the pores form the continuous "phase" (Fig. 2c). The fractured material can be found as isolated islands surrounded by the pore system. Due to the local deformation mechanism in the sintering neck, mainly ductile shear fractures are formed (5). If a profile perpendicular to the fracture surface is studied (Fig. 2a), the isolated islands of material are seen as local crack elements connecting pores along the fracture path. Quantitative measurements on fracture profiles of the fraction of the total crack length passing through the material have been made in an earlier investigation (Bertilsson et al. (10)). The path fraction f through the material was defined as

$$f = \alpha/(\alpha+\beta) \tag{1}$$

where $\alpha$ is the sum of $l_i$:s (Fig. 1a) and $\beta$ is the sum of the lengths of straight line elements through the pores connecting the adjacent local cracks along the main crack profile. The measurements showed that f was 0.24 and 0.36 for the porosity levels 0.16 and 0.10 respectively. This is another strong indication of the preference of the crack to be guided by the pore system since the line fraction through the material along a random line would be 0.84 and 0.90 for the two porosities respectively.

In the profile it can be seen that not just one crack but several micro-cracks are formed independently of each other by fractures of relatively "small" sintering necks in the plastic zone (cf. Fig 2a). This micro-cracking is cumulated to a damage zone surrounding the crack tip. The crack will, when stopped by a pore, continuously propagate by interlinkage of micro-cracks in the damage zone in front of the main crack via the most loaded sintering neck, independently of the local crack direction. At this pore it will stop due to the blunting effect of the pore on the crack and new micro-cracks will be formed in front of the macroscopic crack. The result of this propagation mechanism is that the crack "chooses" a minimized way through the material in the structure approximately corresponding to the nearest neighbour pore interdistance in the "forward" main propagation direction. In reality the crack way will probably be minimized over some part of the severely damaged plastic zone, i.e the crack will choose a shorter way through the material than that corresponding to the shortest way between consecutive nearest neighbouring pores in the forward direction (cf. Table 1).

The crack initiation phase of a macroscopic fatigue fracture is considered to normally be a large portion of the total lifetime. Applied to porous steels this means that the number of cycles necessary to initiate a new micro-crack in a sintering neck could be larger than the

number of cycles needed to propagate it through that neck (a typical sintering neck is only about 10 $\mu$m). This might be the explanation of the comparatively high resistance against fatigue crack extension found in porous sintered steels (5).

The broad angle distribution of the crack elements implies that one could expect large modus II displacements at the crack tip in PM-materials as demonstrated by Lankford and Davidsson (11), resulting in a pronounced fracture surface induced closure (cf. Wasén (12)). This can not, because of the $K_{max}$-independence of the fracture surface geometry, explain the linear increase of the crack closure level, $K_{cl}$, with $K_{max}$ found in these materials (5). One possible explanation is that a part of the closure effect is due to the increasing number of micro-cracks developed in the process zone with increasing $K_{max}$. This leads to an unloading at the main crack tip, i.e. a micro-crack induced crack tip shielding mechanism.

## CONCLUSIONS

1. The pores constitute the continuous "phase" in fatigue fracture surfaces of a porous sintered steels.
2. A crack propagates approximately from one pore to the nearest neighbouring pore in the forward direction.
3. The main crack is surrounded by a zone of micro-cracks, resulting in unloading of the main crack tip.

## REFERENCES

(1) Karlsson, B. and Bertilsson, I., Scand. J. Metall., Vol. 11, 1982, pp. 267-275.
(2) Exner, H.E. and Pohl, D., Powder Metall. Int., Vol. 10, 1978, pp. 193-196.
(3) Nakamura, M. and Tsuya, K., Powder Metall., Vol. 22, 1979, pp. 101-108.
(4) Crane, L.W. and Farrow, R.J., Powder Metall., Vol. 23, 1980, pp. 198-202.
(5) Bertilsson, I. and Karlsson, B., In Proc. Fatigue '87, EMAS, Warley, 1987, pp. 577-586.
(6) Douib, N., Mellanby, I.J. and Moon, J.R., Powder Metall., Vol. 32, 1989, pp. 209-214.
(7) Bertilsson, I. and Karlsson, B., Powder Metall., Vol. 30, 1987, pp. 183-188.
(8) Karlsson, B. and Wasén, J., In Proc. 7th European Conf. on Fracture, EMAS, Warley, 1988, pp. 573-592.
(9) Karlsson, B. and Wasén, J., In Proc. 7th Intern. Conf. on Fracture, Pergamon Press, Oxford, 1989, pp. 3383-3390.
(10) Bertilsson, I., Karlsson, B. and Wasén, J., Modern Developments in Powder Metallurgy, Vol. 16, 1985, pp. 19-32.
(11) Lankford, J. and Davidson, D.L., Metall. Trans. A, Vol. 14A, 1983, pp. 1227-1230.
(12) Wasén, J., PhD Thesis, 1988, Chalmers University of Technology, Göteborg, Sweden.

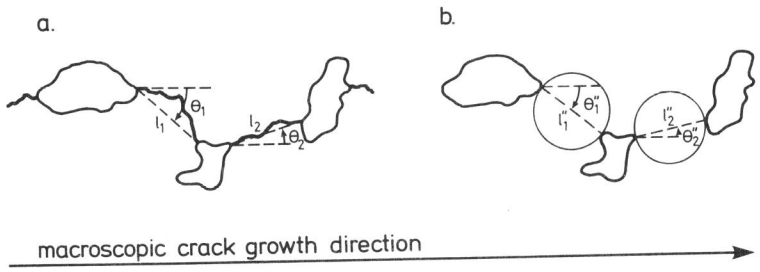


Figure 1 a) Definition of approximation chords used in the fractographic measurements.
b) Definition of approximation chords connecting nearest pores in the "forward" direction (cf. main text).

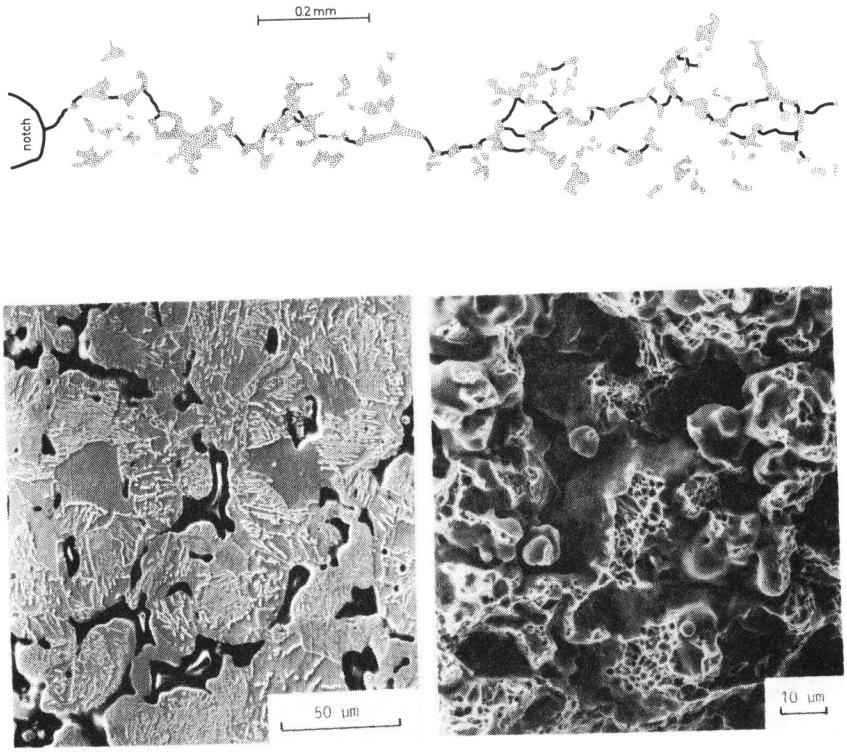


Figure 2 a) Crack pattern reproduced from a specimen with a pore fraction of 0.16.
b) Metallographical section through the material.
c) SEM micrograph of the fracture surface (cf. Fig. 2b).